ELSEVIER

Contents lists available at ScienceDirect

## **Applied Surface Science**

journal homepage: www.elsevier.com/locate/apsusc



## Phase transitions in femtosecond laser ablation

## Mikhail E. Povarnitsyn\*, Konstantin V. Khishchenko, Pavel R. Levashov

Joint Institute for High Temperatures, Russian Academy of Sciences, Izhorskaya 13 Building 2, Moscow, 125412, Russia

#### ARTICLE INFO

Article history:

Available online 12 August 2008

PACS: 61.80.Az 79.20 Ds

64.70.Dv

64.70.Fx

Keywords:
Laser interactions
Laser ablation
Laser melting
Laser-induced spallation

#### ABSTRACT

In this study we simulate an interaction of femtosecond laser pulses (100 fs, 800 nm, 0.1–10 J/cm²) with metal targets of Al, Au, Cu, and Ni. For analysis of laser-induced phase transitions, melting and shock waves propagation as well as material decomposition we use an Eulerian hydrocode in conjunction with a thermodynamically complete two-temperature equation of state with stable and metastable phases. Isochoric heating, material evaporation from the free surface of the target and fast propagation of the melting and shock waves are observed. On rarefaction the liquid phase becomes metastable and its lifetime is estimated using the theory of homogeneous nucleation. Mechanical spallation of the target material at high strain rates is also possible as a result of void growth and confluence. In our simulation several ablation mechanisms are taken into account but the main issue of the material is found to originate from the metastable liquid state. It can be decomposed either into a liquid–gas mixture in the vicinity of the critical point, or into droplets at high strain rates and negative pressure. The simulation results are in agreement with available experimental findings.

© 2008 Elsevier B.V. All rights reserved.

#### 1. Introduction

Ultrashort laser-matter interaction has become the subject of thorough investigations over the past years. Subpicosecond lasers have proved their efficiency in machining, microstructuring, synthesis of nanoparticles, and many other applications. To gain a better understanding of ultrashort nonlinear processes in targets after the laser irradiation a numerical modeling is used. Simulation is based mainly on continual models [1-5] or molecular dynamics [6,7]. The first approach can deal with the real-scale problems. To achieve good agreement with experiment semiempirical models with adjustable coefficients are also used [8]. Nevertheless, continual models have a difficulty of taking into account the micro-level effects such as evaporation, void growths and confluence. On the contrary, molecular dynamics operates with individual atoms and thus reproduces the micro-level mechanisms naturally. The basic problem of molecular dynamics is a choice and adjustment of an interatomic potential that must be in agreement with experimental data for a substance under consideration.

In this work we extend our hydrodynamic approach with kinetic models of evaporation, nucleation, pressure and temperature relaxations to describe the main processes of laser ablation of metals.

## 2. Computational model

In metals the conduction band electrons absorb laser energy in a skin layer and then transmit it into the bulk of the target. At the same time the temperature of the lattice rises due to electron–ion collisions. In this initial stage the temperature of electrons and ions can be essentially different [9].

Our present model is based on the multi-material Eulerian hydrodynamics with separate description of energy for electrons and ions [3,4]. Initially, the target occupies a half-space  $x \geq 0$  and the laser pulse has a Gaussian profile in time. The parameters of the laser pulse are  $\tau_L = 100$  fs,  $\lambda_L = 800$  nm and  $F_L = 0.1-10$  J/cm², where  $\tau_L$ ,  $\lambda_L$  and  $F_L$  are the full width at half maximum of the pulse, wavelength and fluence, respectively. For relatively weak intensities the power density of the laser pulse, absorbed in a skin layer can be approximated by the Beer's law:

$$Q(x,t) = \frac{F_L(1-R)}{\sqrt{\pi/\ln(16)}\tau_L\lambda_{opt}} exp \left[ -\ln\left(16\right) \frac{(t-t_0)^2}{\tau_L^2} \right] exp \left[ \frac{-x}{\lambda_{opt}} \right].$$

Here *R* is the reflectivity, known at particular intensity from the pump-probe experiments [8], *t* is the time  $(t \ge 0)$  and  $t_0 = 5\tau_L$ . Optical penetration depth  $\lambda_{\text{opt}}$  is taken from the experiment [10].

The laser spot size is typically much bigger than the characteristic depth of the heat affected zone (micrometers versus nanometers) and for this reason we can consider the problem in one-dimensional geometry, at least for subnanosecond time

<sup>\*</sup> Corresponding author. Tel.: +7 495 484 2456; fax: +7 495 485 7990. E-mail address: povar@ihed.ras.ru (M.E. Povarnitsyn).

delays. For longer time delays one needs to consider the problem setting in multi-dimensional case.

#### 3. Equation of state

To complete the hydrodynamic equations we use a semiempirical multi-phase equation of state (EOS) with the separate expressions for the subsystems of heavy particles and electrons. The specific Helmholtz free energy has a form  $F(\rho, T_i, T_e) = F_i(\rho, T_i, T_e)$  $T_i$ ) +  $F_e(\rho, T_e)$ . Here  $\rho$  is the material density, while  $T_i$  and  $T_e$  are the temperatures of heavy particles (atoms, ions, nuclei) and electrons, respectively. The first term describes the contribution of heavy particles and the second one gives that of electrons. The ionic term  $F_i$ in turn consists of two parts: the electron-ion interaction part  $F_c$ (calculated at  $T_i = T_e = 0$  K) and the contribution of thermal motion of heavy particles  $F_a$ . The analytical form of  $F_i$  has different expressions for the solid, liquid, and gas phases. Our EOS contains information about phase boundaries which are determined from the equality conditions for the temperatures  $T_i$ , pressures  $P_i = \rho^2 (\partial F_i / \partial \rho)_T$ , and Gibbs potentials  $G_i = F_i + P_i/\rho$  for each pair of phases. Tables of thermodynamic parameters are calculated taking into consideration the information about the phase transitions and metastable regions [11,12]. The free energy of electrons in metal  $F_e$  has a finitetemperature ideal Fermi-gas form [13].

#### 4. Treatment of metastable states

In our model a special treatment of metastable states has been realized. It is known that a subpicosecond laser pulse can result in high-rate isochoric heating (see dashed thermodynamic paths *AB1* and *AB2* in Fig. 1) followed by the rarefaction of a substance (paths *B1C1* and *B2C2* in Fig. 1). On the rarefaction the thermodynamic pathway can cross the liquid branch of the binodal and enter into the metastable region (*C1D1* and *C2D2* in Fig. 1). The lifetime of the metastable state decreases exponentially in the vicinity of the spinodal because of the avalanche-like growth of bubble population. The typical space and time scales of nucleation are nanometers and picoseconds, and this process can be far from thermodynamic equilibrium. To remedy this problem additional kinetic models should be applied.

We consider the homogeneous nucleation as the basic mechanism of metastable liquid separation. It is assumed, that the nucleation process has three basic stages: (i) spontaneous appearance of critical size gas bubbles in liquid, (ii) growth of these

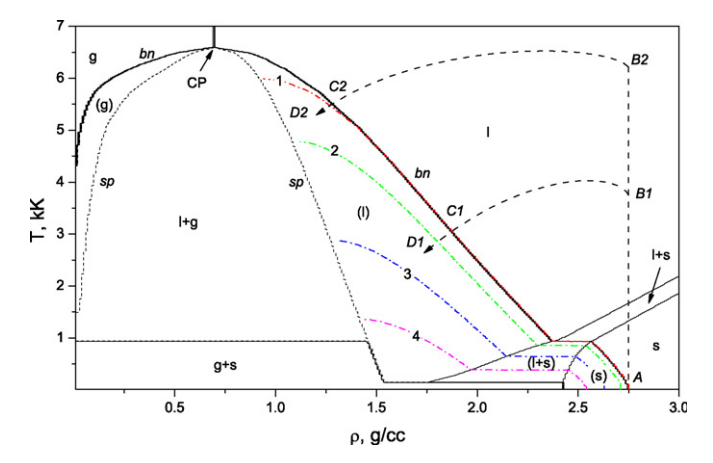


**Fig. 1.** Phase diagram of aluminum. Here sp: spinodal; bn: binodal; g: stable gas; l: stable liquid; s: stable solid; l+s: stable melting; l+s: liquid-gas mixture; g+s: sublimation zone; (g): metastable gas; (l): metastable liquid; (l+s): metastable melting; (s): metastable solid; CP: critical point. Dash-dot lines: isobars; l+s: l+s:

bubbles, and (iii) confluence of bubbles and final relaxation of pressure and temperature.

The first stage can be described by the critical bubble waiting time  $\tau = (J_1 \upsilon)^{-1}$  [14], where  $J_1$  is the nucleation rate and  $\upsilon$  is the volume under consideration. The stability and growth of a new bubble is governed by the condition:

$$P^{\mathrm{g}} > P^{\mathrm{l}} + \frac{2\sigma}{r}$$

where  $P^{\rm g}$  and  $P^{\rm l}$  are the pressures in the gas bubble and liquid, respectively, r is the radius of the bubble and  $\sigma$  is the surface tension. The nucleation rate has a general form [14]:

$$J_1 = Cn \exp\left(\frac{W_c}{k_B T}\right),\,$$

where  $C \approx 10^{10} \, \mathrm{s}^{-1}$  is the kinetic coefficient [15], n is the concentration,  $W_c$  is the work to create a bubble of critical radius and  $k_{\rm B}$  is the Boltzmann constant. The work of the critical bubble formation can be derived as [14]:

$$W_{\rm c} = \frac{16\pi\sigma^3}{3{(P^{\rm g}-P^{\rm l})}^2}. \label{eq:wc}$$

For bubbles of a nanometric radius the surface curvature contributes a lot into the mechanical balance and thus an appropriate wide-range expression for the surface tension is needed. Dependencies known from literature describe the surface tension mainly in the vicinity of the critical or triple points, ignoring the large area in the metastable liquid state where pressure is negative, see region below isobar 1 in Fig. 1. Keeping in mind the fact that the surface tension must tend to zero on the spinodal and knowing the experimental value at the melting temperature we can extend the Eötvös's law for liquid metals into the metastable liquid state:

$$\sigma(T,\rho) = \sigma_0 \left( \frac{T_{\rm c} - T}{T_{\rm c} - T_0} \right) \left( \frac{\rho_{\rm bn}^{\rm l}(T) - \rho_{\rm bn}^{\rm g}(T)}{\rho_{\rm bn}^{\rm l}(T_0) - \rho_{\rm bn}^{\rm g}(T_0)} \right)^{2/3} \left( \frac{\rho - \rho_{\rm sp}^{\rm l}(T)}{\rho_{\rm bn}^{\rm l}(T) - \rho_{\rm sp}^{\rm l}(T)} \right)^{1/2}.$$

Here  $T_c$  is the temperature in the critical point,  $\sigma_0$  is the surface tension in the triple point at temperature  $T_0$ ,  $\rho_{\rm bn}^{\rm l}(T)$  and  $\rho_{\rm bn}^{\rm g}(T)$  are the densities on the liquid and gas branches of the binodal, respectively, and  $\rho_{\rm sp}^{\rm l}(T)$  is the density on the liquid branch of the spinodal. The growth of bubbles on the second stage is governed by the pressure gradient. On the third stage the confluence of bubbles results in the final lost of uniformity by the liquid and formation of a stable two-phase liquid–gas mixture.

### 5. Model of evaporation

We use the model of Hertz–Knudsen [16] to calculate the mass flow of atoms leaving the unit surface during the unit time,  $J_{\rm evap}=P_{\rm bn}^{\rm g}\sqrt{m/2\pi k_{\rm B}T}$ .

Here  $\overrightarrow{P}_{\rm bn}^{\rm g}$  is the pressure of the saturated gas (pressure at the binodal) at temperature T of the condensed phase. Taking into account the back flux in the form  $J_{\rm cond} = P^{\rm g} \sqrt{m/2\pi k_{\rm B} T^{\rm g}}$  we can estimate the total volume fraction of evaporated or condensed substance on the surface S in any volume of interest  $\upsilon$  during the time  $\Delta t$  as follows:

$$f_{\mathrm{evap}} = (J_{\mathrm{evap}} - J_{\mathrm{cond}}) \frac{S\Delta t}{(\rho^{\mathrm{l}} v)}.$$

The negative value of  $f_{\rm evap}$  indicates that the condensation process predominates.

We adopt the procedures of pressure and temperature relaxation in any multi-phase cell of the size  $\Delta x$  using the relaxation law  $\mathrm{d}P/\mathrm{d}t = -(P-P_\mathrm{eq})/\tau_\mathrm{mech}$ ,  $\mathrm{d}T/\mathrm{d}t = -(T-T_\mathrm{eq})/\tau_\mathrm{therm}$ . Here  $\tau_\mathrm{mech} \approx \Delta x/c_\mathrm{s}$  and  $\tau_\mathrm{therm} \approx \Delta x^2/\chi$  are the mechanical and

## Download English Version:

# https://daneshyari.com/en/article/5367506

Download Persian Version:

https://daneshyari.com/article/5367506

<u>Daneshyari.com</u>